A practical study of the aerodynamic impact of wind turbine blade leading edge erosion

N Gaudern

Vestas Technology UK Ltd.
West Medina Mills, Stag Lane, Newport, Isle of Wight, PO32 5TS

E-mail: nigau@vestas.com

Abstract. During operation wind turbine blades are exposed to a wide variety of atmospheric and environmental conditions; inspection reports for blades that have been operating for several years show varying degrees of leading edge erosion. It is important to be able to estimate the impact of different stages of erosion on wind turbine performance, but this is very difficult even with advanced CFD models. In this study, wind tunnel testing was used to evaluate a range of complex erosion stages. Erosion patterns were transferred to thin films that were applied to 18% thick commercial wind turbine aerofoils and full lift and drag polars were measured in a wind tunnel. Tests were conducted up to a Reynolds number of 2.20×10^6, and scaling based on the local roughness Reynolds number was used in combination with different film thicknesses to simulate a variety of erosion depths. The results will be very useful for conducting cost/benefit analyses of different methods of blade protection and repair, as well as for defining the appropriate timescales for these processes.

1. Introduction

During operation wind turbine blades are exposed to a wide variety of atmospheric and environmental conditions; inspection reports for blades that have been operating for several years show varying degrees of leading edge erosion. The scale and form of erosion features develop over time, with the observed damage ranging from small pin holes to a substantial loss of leading edge paint. [1-4] The erosion of blade leading edges is considered to be normal wear and tear.

Vestas is actively looking at preventive solutions and repair methods for LE erosion. This study forms part of that work, since it is essential that the impact of different stages of erosion on wind turbine performance may be estimated with confidence, so that appropriate cost-benefit analyses can be carried out to assess the different methods of protection and repair. The potential impact of erosion also needs to be understood so that appropriate steps can be taken during the aerofoil design process to mitigate its effects. Wind tunnel testing was chosen as the quickest and most effective method of evaluating a range of complex erosion stages; there is no well-established method for CFD simulation of such issues. [5]

2. Construction and scaling of LE erosion patterns

Inspection reports and photographs of Vestas turbines that have been operating for up to 5 years were used to assemble a collection of different types of LE erosion, a sample from which is given in Figure 1. Using this information, five categories of severity were identified visually, and are described in Table 1.

Table 1. LE erosion category descriptions.

Erosion category	Description
1	Small pin-holes of missing paint distributed across LE with some grouping
2	Pin-holes have coalesced in to larger eroded patches
3	Affected area has increased, with isolated larger patches with a greater depth
4	Patches have coalesced further and depth has increased
5	Large areas of LE laminate exposed

Approximate dimensions of erosion features were taken from the inspection reports and combined with scaling from photographs to assign a representative diameter, depth, and chordwise extent for each erosion category (Table 2), which was used to design a simplified pattern to represent each erosion stage. Figures 2-6 show the different erosion stages that were designed. When compared to the source photographs, the patterns represent well the defining features of the erosion, but are more uniform in nature and do not capture the erosion features and roughness that has a high spatial frequency. The different erosion patterns were transferred to thin self-adhesive foils by water-jet cutting.

Table 2. LE erosion pattern dimensions.

Erosion pattern	Erosion depth (mm)	Average feature diameter (mm)	Approx. % chord coverage
1	0.1-0.2	2	3
2	0.1-0.2	15	3
3	0.3-0.5	20/40	5
4	0.5-0.8	40	5
5	0.8-1.2	>500	8

Figure 1. Examples of LE erosion.

Figure 2. Stage 1 erosion.

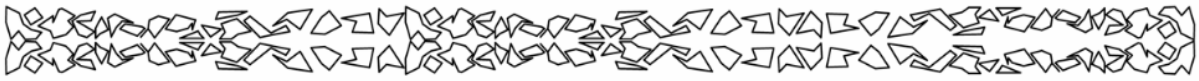

Figure 3. Stage 2 erosion.

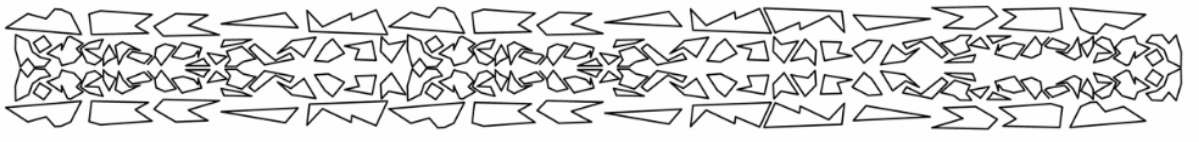

Figure 4. Stage 3 erosion.

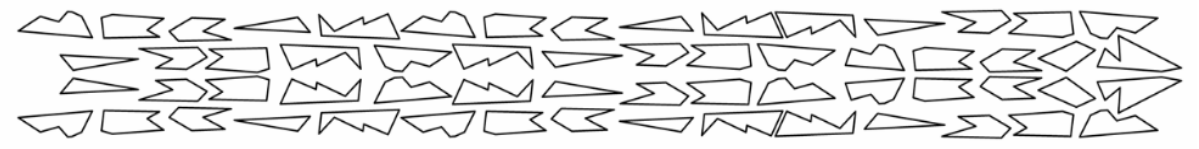

Figure 5. Stage 4 erosion.

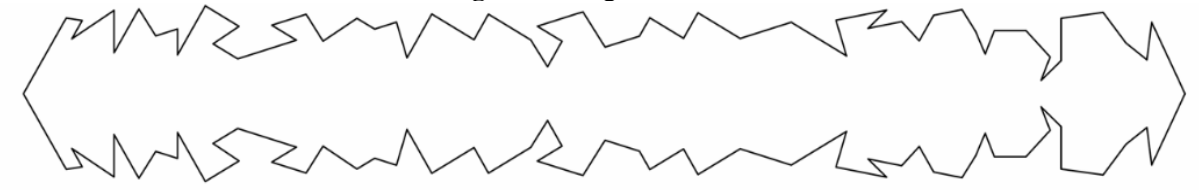

Figure 6. Stage 5 erosion.

2.1. Scaling parameter

A limited number of appropriate foils with different depths were available for testing (0.23mm, 0.36mm, 0.60mm, and 1.50mm). To test LE erosion patterns at the desired effective depths at full-scale Reynolds numbers, and to minimise the number of foils required for testing, a suitable scaling parameter had to be chosen for the erosion depths. The parameter chosen was the Reynolds number based on the size of boundary layer roughness features. [5,6]

$$\mathrm{RE}_k = \frac{\rho u(k) k}{\mu} \tag{1}$$

where ρ is the density, $u(k)$ is the velocity at the roughness height, k is the roughness height, and μ is the dynamic viscosity.

Close to the surface, where it can be assumed that the boundary layer velocity gradient varies linearly with height, $u(k)$ can be written as:

$$u(k) = \frac{k\tau_\omega}{\mu} \tag{2}$$

where τ_ω is the wall shear stress, which can be found using *XFOIL* for the clean aerofoil. [7] *XFOIL* outputs the value of the skin friction coefficient – *CF* – from which τ can be found by multiplying by $0.5*\rho*U^2$, where *U* is the free-stream velocity. *XFOIL* input conditions were as follows: number of panels, 180; default panel bunching and density ratios; N-value, 9.

With this definition of *u(k)*, RE_k can be written as follows:

$$RE_k = \frac{\rho k^2 \tau_\omega}{\mu^2} \tag{3}$$

This formula can be used to calculate the appropriate test Reynolds number when the available foil thickness is different from that required. Assuming test conditions remain constant, then:

$$k^2{}_{test}\tau_{\omega test} = k^2{}_{ref}\tau_{\omega ref} \tag{4}$$

XFOIL was used to find the relationship between τ_ω and RE for the two aerofoils. Substituting for τ_ω gives:

$$\frac{RE_{test}{}^{1.5}}{RE_{ref}{}^{1.5}} = \frac{k^2{}_{ref}}{k^2{}_{test}} (= k^2{}_{ratio}) \tag{5}$$

which can be re-arranged to give the following expression, with the reference RE set to be 3 million. On a wind turbine rotor greater than 100m in diameter, the Reynolds number at the tip of the blade (>95% span) is approximately 3 million.

$$RE_{test} = EXP\left(\frac{\ln(k^2{}_{ratio} \times 3e6^{1.5})}{1.5}\right) \tag{6}$$

3. Test conditions

The tests were performed in the Laminar Wind Tunnel (LWT) of the 'Institute for Aerodynamics and Gasdynamics' (IAG), University of Stuttgart. [8] The LWT is an open return tunnel with a closed test section. The rectangular test section measures 0.73m^2 x 2.73m^2 and is 3.15m long. The tunnel has a very low longitudinal turbulence level of 2x10^{-4} to 5x10^{-4}. A 2D aerofoil model spans the short distance of the test section; gaps between model and tunnel walls are sealed. For each LE erosion pattern a full lift and drag polar including post-stall was measured; an AoA range of -16° to +16° was sufficient to capture the positive and negative post-stall behaviour for every test configuration. The boundary layer transition position was determined by stethoscope and infrared images. Lift was determined by integration of the pressure distribution along the opposite two tunnel walls, and drag was determined by an integrating wake rake positioned approximately 0.45 x chord length behind the model trailing edge.

Two aerofoils were tested: the first was an 18% thick proprietary Vestas section, and the second was an 18% thick Risø section; both aerofoils are used on modern wind turbines. Both aerofoil models had a chord length of 600mm. The 18% aerofoil is found towards the tip section of the blades where LE erosion is most pronounced.

The test matrix is given in Table 3. It can be seen that some of the effective test depths achieved did not fall precisely within the target range; this was due to compromises when optimising the test matrix to minimise the number of Reynolds number/foil depth configurations used (in addition to the erosion tests, the same test campaign investigated other surface defects requiring specific Reynolds numbers).

Table 3. Wind tunnel test matrix.

Erosion pattern	Aerofoil	Target depth (mm)	Film thickness (mm)	Effective test depth (mm)	Reynolds number (x10^6)	Mach number
1	Vestas	0.1-0.2	0.23	**0.18**	2.20	0.16
1	Risø	0.1-0.2	0.23	**0.17**	2.05	0.15
2	Vestas	0.1-0.2	0.23	**0.18**	2.20	0.16
2	Risø	0.1-0.2	0.23	**0.17**	2.05	0.15
3	Vestas	0.3-0.5	0.36	**0.28**	2.20	0.16
3	Vestas	0.3-0.5	0.60	**0.48**	2.20	0.16
3	Risø	0.3-0.5	0.36	**0.27**	2.05	0.15
4	Vestas	0.5-0.8	0.60	**0.48**	2.20	0.16
4	Risø	0.5-0.8	1.50	**0.75**	1.20	0.09
5	Vestas	0.8-1.2	1.50	**1.00**	1.75	0.13
5	Vestas	0.8-1.2	1.50	**1.20**	2.20	0.16
5	Risø	0.8-1.2	1.50	**0.75**	1.20	0.09

Figure 7 shows a model installed in the tunnel.

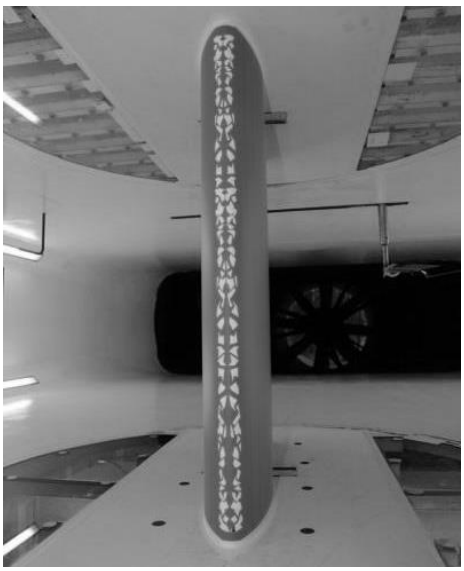

Figure 7. Aerofoil model installed in wind tunnel with LE erosion pattern 2 applied.

3.1. Reference measurements

For both aerofoils and at every test Reynolds number, a lift-drag polar was measured for the clean wind tunnel model. Some of the erosion test depths required the use of 1.5mm thick silicone foil; due to its thickness, reference measurements were made with a blank foil covering the entire aerofoil.

A standard practice for evaluating the performance impact of roughness on an aerofoil is to use LE trip devices to force the flow to transition to turbulence at a given location. [5] In addition to the clean reference measurements, a lift/drag polar was measured for each test condition with the LE tripped at 5% chord using plastic self-adhesive zig-zag tape (0.38mm depth with 60° opening angle).

4. Test results

The results of the tests are presented by erosion stage for both aerofoils, and have been normalised by the appropriate clean reference data for each test condition. In addition to the erosion results the impact of the tripped LE reference runs are presented on the same chart. The x-axis of each chart represents the aerofoil's angle of attack and results are presented between 0° and 8°, which covers the typical operating range of the aerofoils on the turbine. The left-hand y-axis represents the normalised drag data, and the right-hand y-axis the normalised lift data.

4.1. Erosion stage 1

The normalised results for erosion stage one with 0.17mm and 0.18mm depth are given in Figure 8. Both aerofoils suffer a reduction in lift and increase in drag at all angles of attack between 0° and 8°. Apart from at 8°, the drag increase for both aerofoils is lower for the eroded case than the tripped case.

4.2. Erosion stage 2

The normalised results for erosion stage two with 0.17mm 0.18mm depth are given in Figure 9. Both aerofoils show degradation in performance compared to the stage one erosion tests. The mean reduction in lift and increase in drag is still lower than that of the tripped case.

4.3. Erosion stage 3

The normalised results for erosion stage three with 0.28mm and 0.48mm depth are given in Figure 10. Both aerofoils show degradation in performance compared to the stage two erosion tests. When the erosion depth on the Vestas aerofoil is increased from 0.28mm to 0.48mm, the drag penalty increases by approximately 10% over much of the AoA range. This shows that increased erosion depth has a detrimental effect. The mean reduction in lift and increase in drag is now higher than that of the tripped case.

4.4. Erosion stage 4

The normalised results for erosion stage four with 0.48mm and 0.75mm depth are given in Figure 11. Both aerofoils show degradation in performance compared to the stage three erosion tests. The drag increase for both aerofoils is very similar despite the different erosion depths. Based on the previous observations of the Risø aerofoil showing slightly lower drag penalties at higher angles of attack, and the fact that a greater erosion depth in stage three gave a larger drag penalty, it would seem sensible to assume that again, a greater erosion depth for stage four will result in a greater drag penalty.

4.5. Erosion stage 5

The normalised results for erosion stage five with 0.75mm, 1.0mm, and 1.2mm depth are given in Figure 12. Despite being the most advanced stage of erosion, the drag penalties are not the greatest; the 0.75mm depth gives a similar result to the 0.28mm depth stage three, and at higher angles of attack the 1.0mm and 1.2mm depths are not as severe as either of the stage four erosion depths. A possible explanation is that the LE of the aerofoil is still very smooth before the step of the erosion is reached; therefore the impact on the boundary layer will not be as great as when there are erosions pits all the way to the LE. A better approach to testing the stage five erosion may have been to apply one of the previous patterns to the very LE of the aerofoil, so as to roughen the surface prior to the main step. The results for the 1.0mm and 1.2mm depths are very similar, suggesting that there might be a critical depth for this type of erosion, beyond which further drag increase is negligible. Another possible explanation could be that the increase in roughness depth from 1.0mm to 1.2mm as a percentage increase is small compared to the other increases in depth (i.e. 0.75mm to 1.0mm).

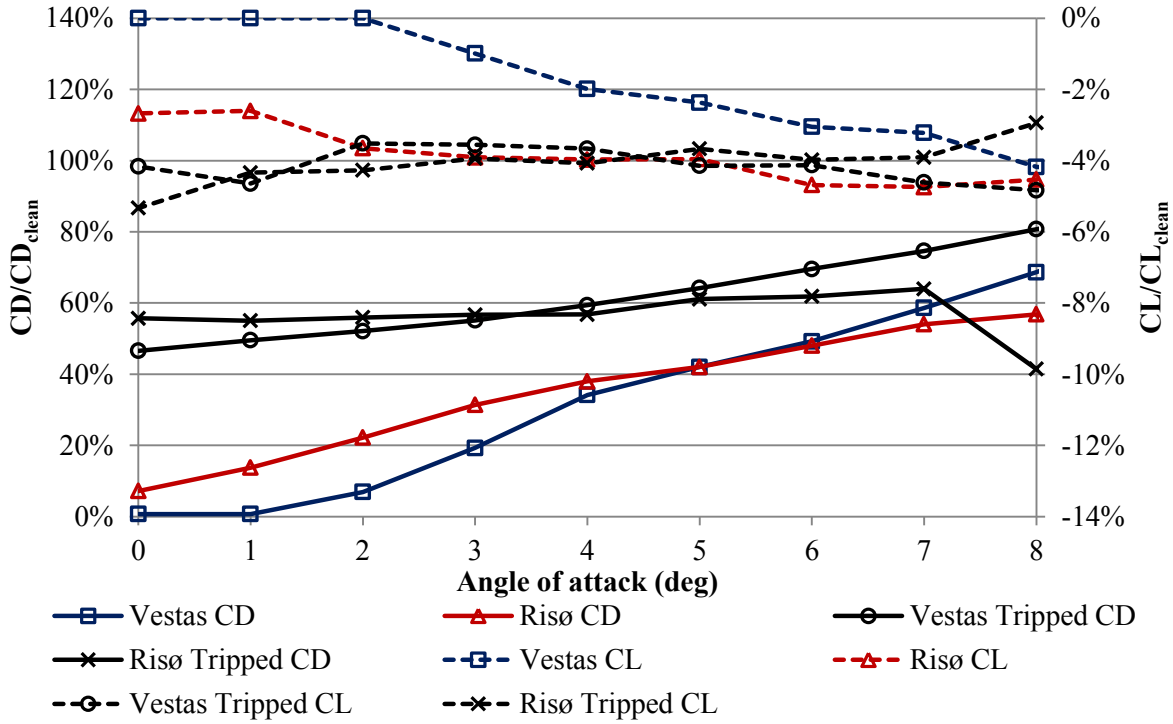

Figure 8. Normalised lift and drag data for erosion stage 1.

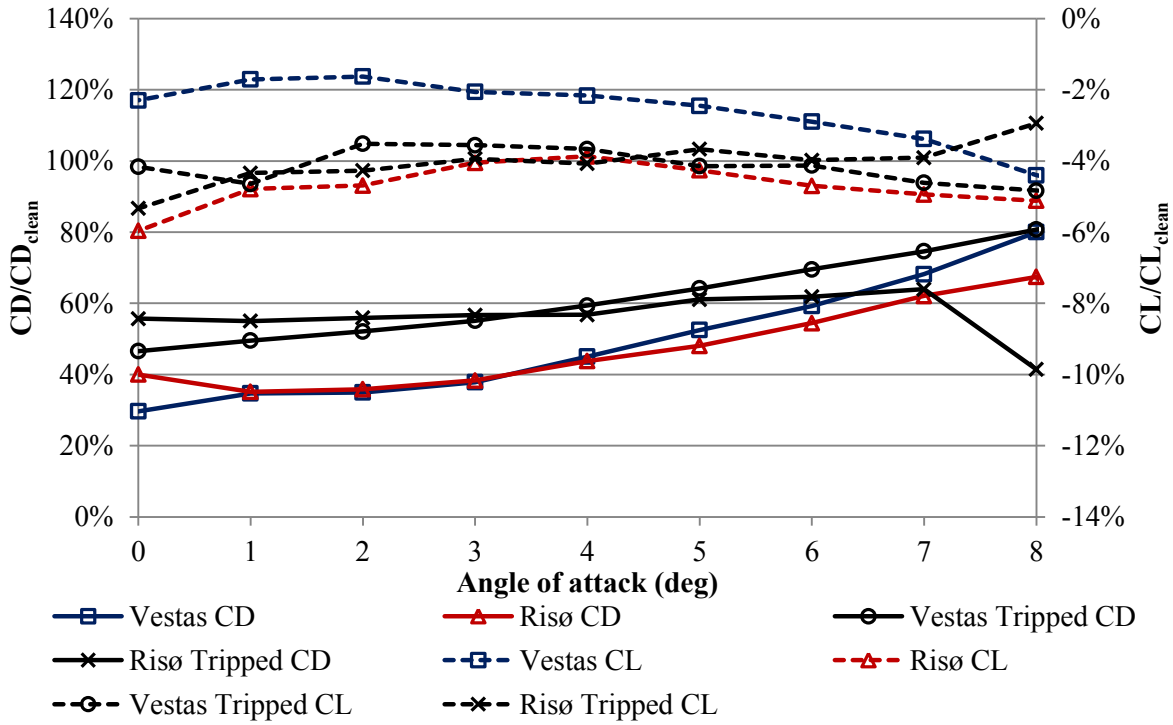

Figure 9. Normalised lift and drag data for erosion stage 2.

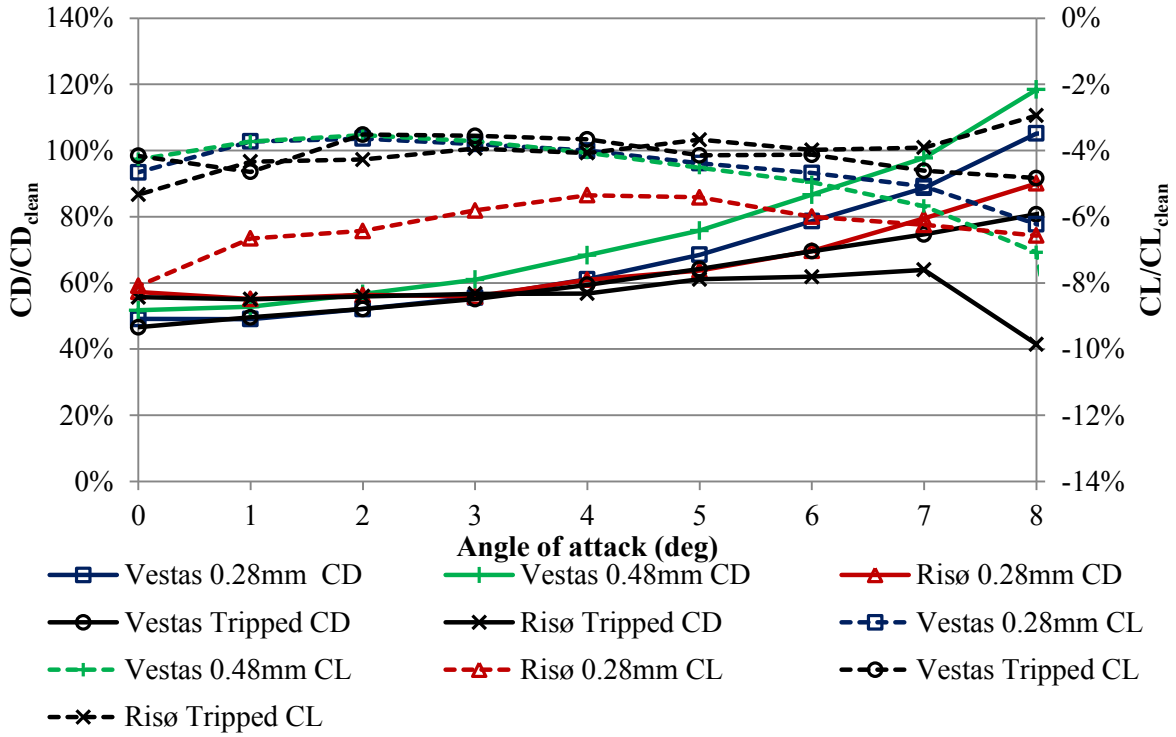

Figure 10. Normalised lift and drag data for erosion stage 3.

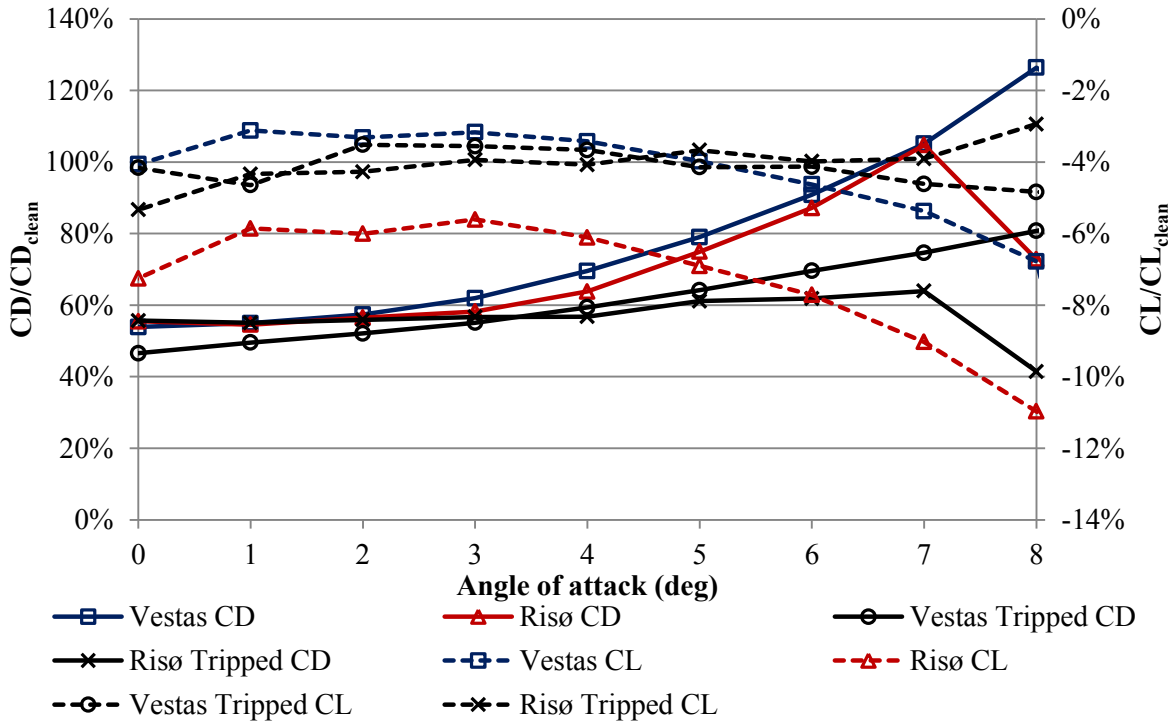

Figure 11. Normalised lift and drag data for erosion stage 4.

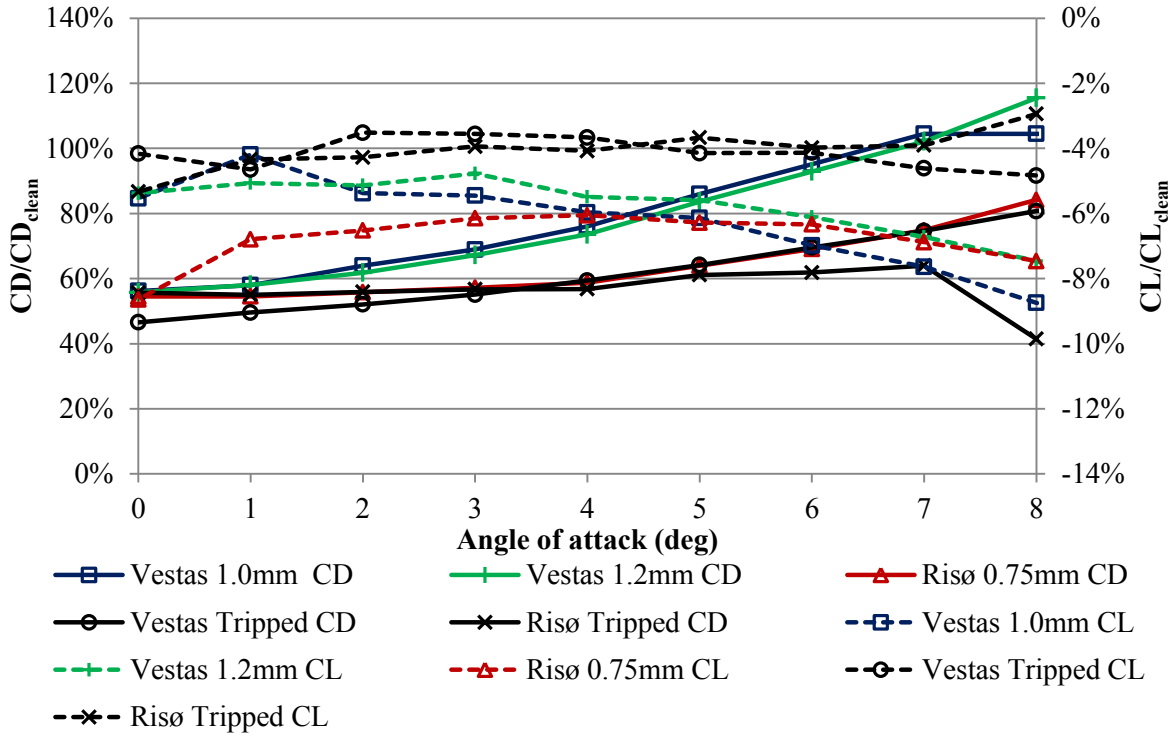

Figure 12. Normalised lift and drag data for erosion stage 5.

4.6. Summary of results

Table 4 summarises the lift and drag penalties at a single angle of attack (representative operating point of 6°), averaged over both aerofoils and any variations in test depth. A clear trend is visible: with greater levels of erosion both the lift reduction and drag increase is more severe (excepting the drag increase for stage 5, discussed previously). These figures could be used to carry out a simplified performance analysis of an eroded wind turbine blade.

The tripped LE test case gives lift reductions the same as those in the least severe erosion cases, and drag increases approximately halfway between the smallest and largest increases recorded. The results suggest that a tripped LE gives representative results if being used to simulate LE erosion; however, the results will not be conservative, and at higher angles of attack the difference between the eroded case and tripped case was shown to increase further.

Table 4. Summary of test results at AoA of 6°.

Erosion pattern	Average CL decrease @ AoA=6°	Average CD increase @ AoA=6°
Tripped	4%	66%
1	4%	49%
2	4%	57%
3	5%	78%
4	6%	89%
5	6%	86%

Table 5 summarises the lift-to-drag ratio (L/D) reductions calculated for each aerofoil when the same erosion depth was tested on both aerofoils. Under clean conditions, the Vestas aerofoil has an

approximately 7% better L/D than the Risø aerofoil; the table shows that when both are eroded, the performance reduction of the two aerofoils is very similar.

Table 5. Summary of L/D reduction at AoA of 6°.

Erosion pattern	Risø	Vestas
1	36%	35%
2	38%	39%
3	45%	47%

5. Conclusions

Two modern, commercial 18% thick wind turbine-specific aerofoils were tested with a variety of LE erosion patterns with varying depths. The erosion configurations were designed by scaling photographs and using inspection reports from real-world wind turbines of different ages. Full lift and drag polar measurements were recorded.

All erosion configurations degraded the performance of both aerofoils by reducing lift and increasing drag. Apart from the described exceptions, as the pattern severity/depth of the erosion increased the aerofoil performance decreased. The performance trends of the two aerofoils were comparable, but there were notable differences in whether the erosion had a greater influence on lift or drag.

The use of LE tripping with a zig-zag strip was shown to give aerofoil performance reductions that were comparable to that of the LE erosion test cases; however, the more severe erosion cases degraded the performance considerably more than the tripped case. It is recommended that LE tripping is only used as a guide to predict the impact of LE erosion.

By testing the impact of LE erosion of two different aerofoil designs, it is clear that an aerofoil designer can make decisions about shape that lead to a better overall design, i.e. higher L/D under both clean and eroded conditions.

References

[1] Keegan M H, Nash DH and Stack M M 2013 On erosion issues associated with the leading edge of wind turbine blades *J. Phys. D: Appl. Phys.* **46** 383001

[2] Dalili N, Edrisy A and Carriveau R 2009 A review of surface engineering issues critical to wind turbine performance *Renewable and Sustainable Energy Reviews* **13**, 428-38

[3] Chinmay S 2012 Turbine blade erosion and the use of wind protection tape (*Masters Thesis) University of Illinois*

[4] Rempel L 2012 Rotor blade leading edge erosion – real life expereinces *Wind Systems Magazine* **October**

[5] Ehrmann R S, White E B, Maniaci D C, Chow R, Langel C M, Van Dam C P Realistic leading-edge roughness effects on airfoil performance *31st AIAA Applied Aerodynamics Conf.* Jun 2013 San Diego

[6] White E B, Kutz D, Freels J, Hidore J P, Grife R, Sun Y, Chao D Leading-edge roughness effects on 63_3-418 airfoil performance *49th AIAA Aerospace Sciences Meeting* Jan 2011 Orlando

[7] Drela M, Youngren, H, XFOIL Subsonic Airfoil Development System [Online] Available:http://web.mit.edu/drela/Public/web/xfoil/, VER 6.97

[8] Technical description of Stuttgart IAG Laminar Wind Tunnel [Online]. Available: http://www.iag.uni-stuttgart.de/IAG/institut/abteilungen/laminarwindkanal/info_laminar_wind_tunnel.htm. [Accessed March 2013]